Study of variation of pore properties in gravel soil under triaxial loading based on discrete element method

Jun Yu[1,2], Chang Jiang Wu[1,*], Chaojun Jia[3] and Weiya Xu[2]

[1]School of Transportation and Civil Engineering, Nantong University, Nantong, China
[2]Research Institute of Geotechnical Engineering, Hohai University, Nanjing, China
[3]School of Civil Engineering, Central South University, Changsha, China

Gravel soil is a complex porous medium, whose mechanical behaviour under triaxial loading can be well simulated using the discrete element method. However, numerical simulation of porous medium under compression requires not only the stress–strain behaviour, but also the variation of pore properties. In this study, models of gravel soil with different gravel contents (weight percentage of gravel in gravel soil) are generated by the single particle delivery method, and numerical triaxial tests are performed on these gravel soil samples. The equivalent porosity and equivalent pore size are introduced as evaluation indexes of pores to study the variation of pore properties in the numerical tests. The numerical results indicate that the porosity of gravel soil shows a V-shaped trend with the gravel content, and the gravel soil samples have minimum porosity in the yield stage.

Keywords: Discrete element method, gravel soil, porosity, porous medium, triaxial loading.

GRAVEL soil is a complicated granular material system composed of abundant discrete particles such as coarse-grained soil, grit and gravel. It is also a commonly used filling material for roadbed and earth-rock dam projects[1]. These gravel soils are subjected not only to long-term loads, but also infiltration. Therefore, it is necessary to have strong mechanical properties and good permeability of gravel soil. Engineering practices have shown that engineering disasters were mainly induced by the weakening of the mechanical properties of geotechnical materials due to the infiltration of water[2,3]. As a porous medium, the physical and mechanical properties of gravel soil are strongly affected by pore properties such as pore size, porosity and pore structure[4]. In addition, the pore properties also affect the permeability of gravel soil; fluid flow occurs within inter-connected pores, which govern seepage, drainage, consolidation and internal stability[5]. Therefore, it is essential to study the variation of pore properties of gravel soil in the loading process[6].

*For correspondence. (e-mail: 15921360161@163.com)

During the last decades, considerable efforts have been made to study the mechanical behaviour of gravel soil using numerical simulations[7–10]. Especially, the discrete element method (DEM), which provides an alternative approach to deal with this problem, is gaining popularity in recent years. To accurately represent the gravel with arbitrary shapes embedded in the gravel soil, digital image processing technology[11], non-overlapping spheres packing[12] and overlapping spheres packing[13] were developed, and the meso-structure model of gravel soil has been developed efficiently[14,15]. However, these methods do not involve the description of pore properties of gravel soil, and pore space modelling is still a challenge for DEM. The pore geometries of gravel soil are so complex that they cannot be characterized using non-idealized computational methods[16]. More recently, some novel methods have been proposed to evaluate the pore properties of granular material. For example, some researchers regarded the granular material formed by particle packing as ideal fractal structures, and on this basis, the permeability or soil–water characteristics were studied[17–19]. The digital image processing approaches were also used to study pore properties, e.g. Delaunay tessellation method[20], medial axis method[21] and watershed-based method[22]. However, each of these approaches has limitations. For example, the Delaunay tessellation method can only be applied to pores with no more than four surrounding particles. In the medial axis method, the medial axis of the pore structure needs to be extracted first, and it is difficult to extract the medial axis of a complex pore structure. In the watershed method, the pore structure needs to be converted into the Euclidean distance field, which has a relatively large computational cost. In addition, in such complex methods mentioned above, it is impossible to evaluate the pore properties of gravel soil under compression.

In this study, the discrete element models of gravel soil with different gravel contents was first generated using the sphere packing method. The equivalent porosity and equivalent pore size were introduced as evaluation indexes of pore properties in DEM. The evolution of pore properties in the failure process was analysed by the numerical triaxial test.

DEM model of gravel soil

As a development of granular DEM, non-sphere packing is widely used to simulate the gravel soil[12]; the regular-shaped particles represent soils and the irregular-shaped particles represent gravels. The morphological characteristics of gravels can be preferably retained in the discrete element model by non-sphere packing. However, there are two drawbacks in generating the model of gravel soil using non-spherical particles. First, in the initial state of the model, the gravel particles do not have contact with each other, which is inconsistent with the actual situation. Secondly, it is more complicated in calculating the porosity on account of irregular shape of non-spherical particles. Due to the above, spherical particles are used to model the gravel in gravel soil in this study. Earlier, researchers have simulated the mechanical characteristics of gravel soil through spherical particles, and the results prove the effectiveness of the method.

Distribution of particle size in the DEM model

Gravel soil has a size effect, which means that the smallest grain size in gravel soil is determined by the size of the sample. Based on several experiments, Medley[23] concluded that the grain size of gravel in gravel soil ranges from $0.05L_c$ to $0.75L_c$ (L_c is the diameter of the sample of the triaxial test). However, the maximum grain size in gravel soil is generally unfavourably, exceeding one-fifth of the diameter of the triaxial test sample[10]. Therefore, the threshold value of grain size of soil and gravel is determined by the size of the sample. In order to statistically analyse the pore properties in gravel soil, cubic samples are used here for the numerical triaxial. The initial size of the cubic sample is 300 mm × 300 mm × 300 mm, the maximum particle diameter of gravel in the sample is 50 mm and threshold value of the particle diameter of soil and gravel is 10 mm. Seven numerical models with the gravel content of 20%, 30%, 40%, 50%, 60%, 70% and 80% respectively, were generated; Figure 1 shows their grading curves.

Model generation

The single-particle delivery method is used to develop the model, which ensures that the gravel content of the generated numerical model is consistent with the target value. Details of the procedure are as follows:

(1) The gradation of gravel soil in Figure 1 is based on the mass ratio of soil and gravel, which in the numerical model is the volume ratio of the soil and gravel particles. The mass cumulative percentage in Figure 1 should be converted to volume cumulative percentage through the general density ratio of soil and gravel, viz. 1 : 1.25.

(2) Calculate the volume of particles in each particle fraction based on the initial size of the sample (300 mm × 300 mm × 300 mm).

(3) We assume that grain size of the particles in each particle fraction is subject to uniform distribution. The particles are generated one by one in a space of size 1.5 times the initial size of the sample. Particle fractions with smaller grain size followed by larger grain size are generated, until the gradation of the model is consistent with the target gradation.

(4) Compress the space to make all particles come in close contact. Figure 2 *a* shows the compacted sample. Figure 2 *b*–*h* shows the distribution of gravels in samples with seven different gravel contents after compaction respectively. As the amount of gravel increases, the contact between the gravels is stronger.

Micro-contact parameters calibration

The macroscopic deformation of DEM is significantly influenced by the micro-contact parameters because the particles are interconnected by contacts in the granular discrete element model. To calibrate the micro-contact parameters, triaxial test was performed on the gravel soil sample with 20% gravel content in the laboratory. The loading rate was 0.02 mm/min and confining pressure was 100 kPa. Numerical triaxial test was conducted on gravel soil model with the same boundary conditions. According to the contact characteristics of the real gravel soil, the contact model between particles in DEM was selected as the linear contact model (linear model). Table 1 shows the calibrated micro-contact parameters.

Figure 3 shows a comparison between the stress–strain curves of laboratory test and numerical test. It is observed from the figure that the numerical simulation results are

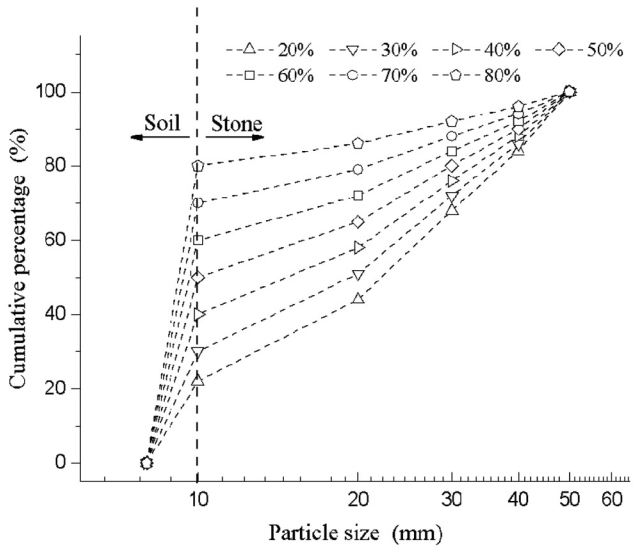

Figure 1. Particle size distribution of the numerical model.

Table 1. Micro-contact parameters between particles in the model

Particle	Density (kg/m^3)	Contact stiffness (N/m)		Friction coefficient
		Normal	Tangential	
Soil	1900	5e5	1.7e5	0.3
Gravel	2650	1e7	3.5e7	0.8
Soil–gravel	–	4.8e5	1.6e5	0.3

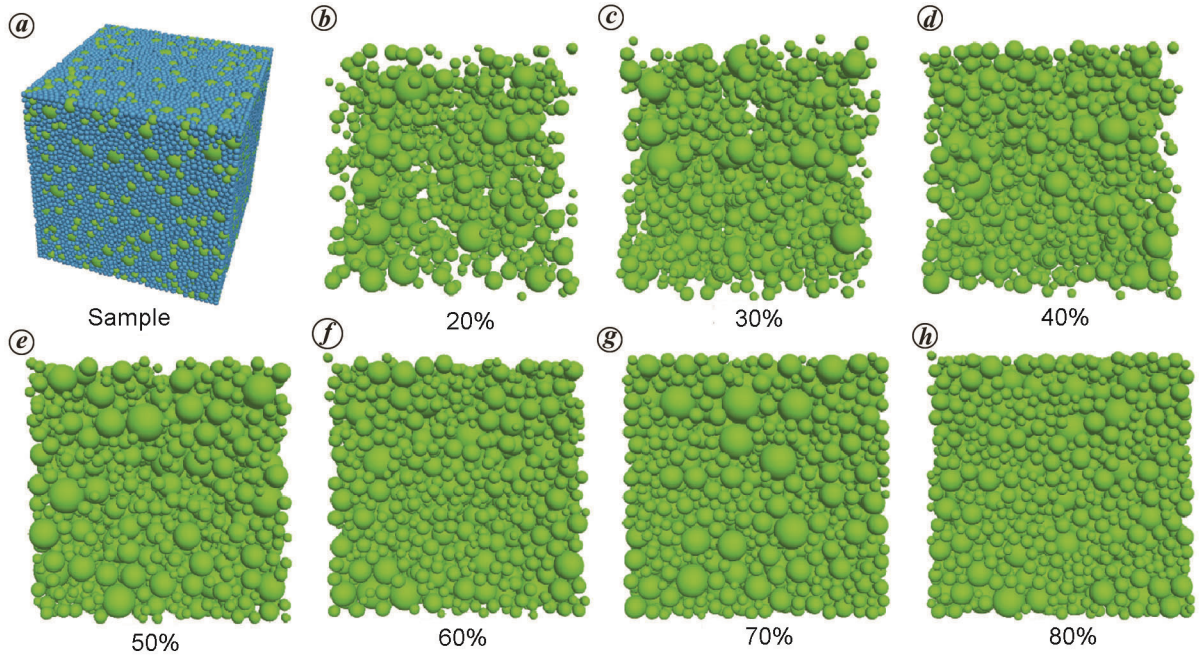

Figure 2. The numerical model and random distribution of gravels in samples with different gravel contents.

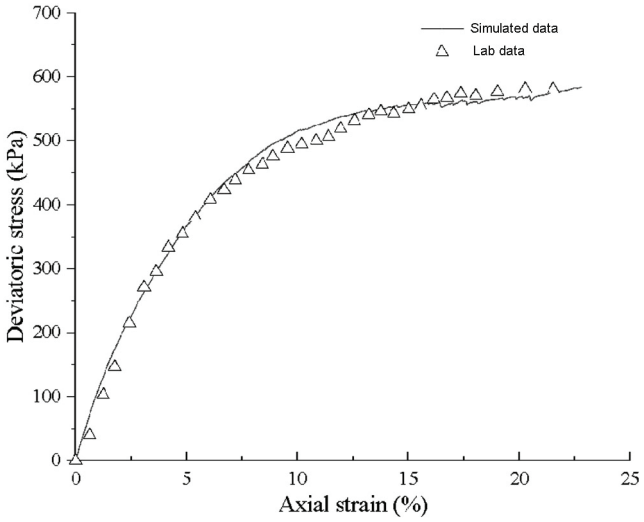

Figure 3. Comparison of stress and strain curves between simulated test and laboratory test.

consistent with the experimental results. The calibrated micro-contact parameters can be used to simulate the variation of pore properties in gravel soil.

The loading process

As shown in Figure 4, the loading model consists of six walls, and the loading process is divided into two stages. (1) The confining pressure ($\sigma_1 = \sigma_2 = \sigma_3$) is applied to the cubic sample by triaxial servo loading, and the maximum loading speed is 0.005 m/s. The porosity and pore size are measured when the confining pressure reaches 100, 200, 300, 400 and 500 kPa respectively. (2) Keep $\sigma_2 = \sigma_3 = 500$ kPa, and apply axial stress at a loading rate of 0.002 m/s until the sample is broken. The porosity and pore size are measured in this loading process.

Parameters of pore properties

Equivalent porosity

In the discrete element model, porosity of the sample is calculated as the ratio of the volume of all pores to the volume of the sample, where the latter is the volume enclosed by the walls, and the volume of all pores is the volume of the sample minus the volume of all particles, excluding the overlapping portion. In Figure 5 *a*, the

overlapping portion of the particles is marked in red. Therefore, the equivalent porosity of gravel soil in the model can be expressed as

$$p = 1 - \frac{V_b - V_o}{V_s}, \tag{1}$$

where V_s is the volume of the cubic sample, that is, the volume enclosed by the walls, V_b the volume of all particles and V_o is the volume of the overlapping portion of all particles.

V_b can be calculated as follows

$$V_b = \sum_{i=1}^{n} \frac{4\pi(r_i)^3}{3}, \tag{2}$$

where n is the total number of particles in the sample and r_i is the radius of the ith particle.

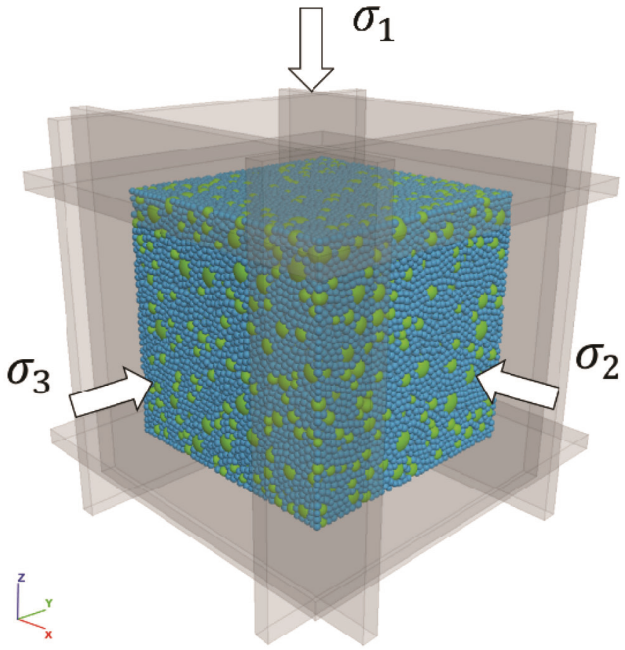

Figure 4. The triaxial loading model.

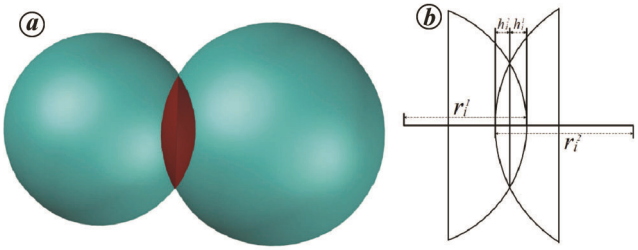

Figure 5. Schematic diagram of the overlapping portion between two particles.

Figure 5 *b* is a schematic diagram of the overlapping portion of two particles. Obviously, the overlapping portion consists of two spherical crowns. Therefore, the volume of the overlapping portion of all particles is expressed as given in eq. (3), which is based on the volume calculation formula of the spherical crown.

$$V_o = \sum_{i=1}^{k} \left(\frac{\pi(h_i^1)^2(3r_i^1 - h_i^1)}{3} + \frac{\pi(h_i^2)^2(3r_i^2 - h_i^2)}{3} \right), \tag{3}$$

where k is the total number of contacts between particles in the sample, r_i^1, r_i^2 are the radii of two particles belonging to the ith contact respectively, and h_i^1, h_i^2 are the heights of the corresponding spherical crowns.

Equivalent pore size

The permeability of a material is closely related to porosity and the pore size, especially pore size has a significant effect on the permeability of gravel soil[24]. The pore size is positively correlated with particle size of gravel. In a constant sized sample, the sizes of particles are larger. Therefore, the number of particles that comprise the sample is less, which means the number of contacts between particles is less. Thus the pore size is negatively correlated with the number of contacts in a constant-sized sample. As it is difficult to evaluate the size of each pore in the sample, an average value ε related to the total volume of pores and the number of contacts can be used to evaluate the average size of pores in the sample, which is expressed as follows

$$\varepsilon = \frac{V_v}{m}, \tag{4}$$

where V_v is the total volume of pores in the sample, which can be calculated from $V_v = V_s - (V_b - V_o)$. m is the number of contacts.

Analysis

Analysis of equivalent porosity

Figure 6 shows the variation of porosity with confining pressure. For samples with the same gravel content, porosity decreases with increase in confining pressure, and the decreasing trend gradually becomes gentle. The variation ranges of porosity of the samples with high gravel content are less. For example, in the process of increasing the confining pressure from 100 to 500 kPa, the porosity of the samples with 80% gravel content decreases by only 7%. In addition, when the confining pressure is more than 300 kPa, the porosity of the samples with 80% gravel content barely changes. In the compression process, the

porosity of the samples with medium gravel content decreases by more than 25%, e.g. samples with the gravel content 50% and 60% whose porosity decreases by 27.2% and 29.7% respectively. The porosity of the samples with low gravel content decreases by more than 30% in the compression process, and the samples remain compressible under higher confining pressure.

Figure 7 shows the variation of porosity with gravel content. It can be concluded from the figure that with the increase in gravel content, the porosity of the gravel soil decreases first and then increases. When the gravel content is less than 50%, there is an approximately linear relationship between porosity and gravel content of gravel soil. When the confining pressure is lower than 200 kPa, the porosity of the 70% gravel-containing sample is the smallest, and the sample is the densest. When the confining pressure exceeds 200 kPa, the porosity of the sample with gravel content of 60% is the smallest. When the confining pressure continues to increase, the sample with 50% gravel content has the smallest porosity.

Figure 8 shows the relationship between porosity of seven types of samples and axial strain under a confining pressure of 500 kPa. It can be observed from the figure that the porosity of all samples shows a V-shaped trend as the axial strain increases. However, in the loading process, the decrement of porosity of samples with high gravel content (70% and 80%) is not obvious. When the axial strain exceeds 2%, the porosity increases significantly, with an increase of about 10% during the whole loading process. When the axial strain exceeds 6%, the porosity of samples with medium gravel content (50% and 60%) increases, by 3% and 6% respectively, during the whole loading process. The porosity of samples with low gravel content (20%, 30% and 40%) decreases significantly, with reduction between 7% and 15% before the turning points. When the axial strain reaches 13–17%, the porosity of samples with low gravel content begins to increase, but eventually fails to exceed the initial porosity.

Figure 9 shows the evolution of deviatoric stress and porosity with axial strain. The corresponding axial strain at minimum porosity is the position after the sample enters the yield stage, which means the gravel soil sample has minimum porosity in the yield stage. Moreover, this property is not affected by the gravel content of the sample. When the sample is in the elastic stage, the compressed pores in it can still be recovered after the load is removed. When the sample enters the yielding stage, some irreversible deformation occurs; new pores are formed and the original pores are still compressed. The porosity of the sample begins to increase when the formation of new pores is greater than the compression of the

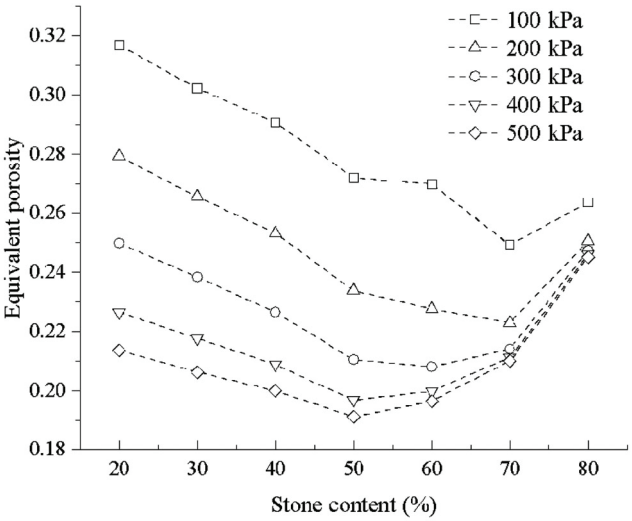

Figure 7. Relationship between equivalent porosity and gravel content.

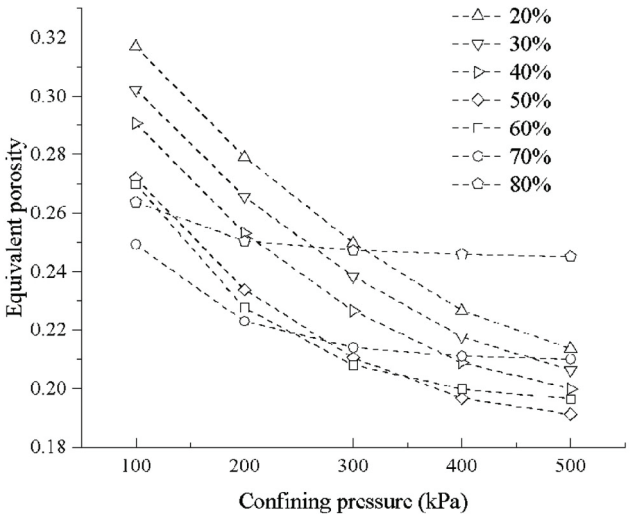

Figure 6. Relationship between equivalent porosity and confining pressure.

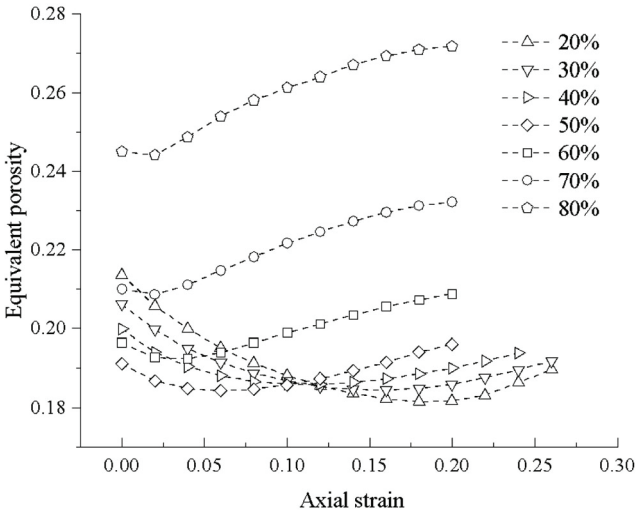

Figure 8. Relationship between equivalent porosity and axial strain.

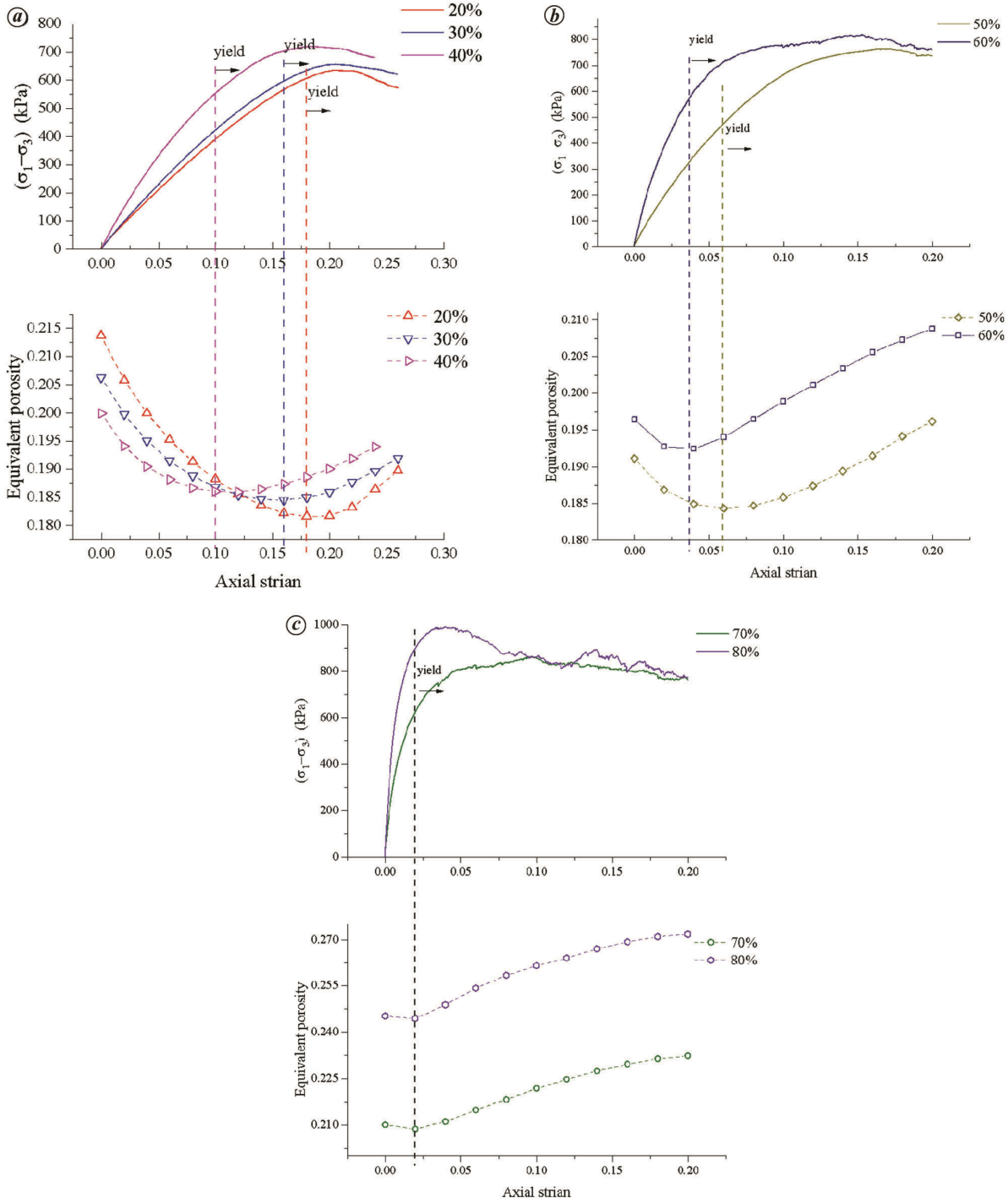

Figure 9. Evolution of deviatoric stress and porosity with axial strain.

original pores. Therefore, the gravel soil sample has minimum porosity in the yield stage.

Analysis of equivalent pore size

Figure 10 presents the variation of average pore size with confining pressure. As the confining pressure increases, the average pore size of all samples decreases. When the confining pressure exceeds 400 kPa, changes in the average pore size are no longer significant. In the process of increasing the confining pressure from 100 to 500 kPa, the average pore size of the samples with low and medium gravel content decreases by more than 50%, but the average pore size of the 70% and 80% gravel content samples decreases by 31.8% and 17.5% respectively.

Figure 11 shows the relationship between average pore size and gravel content. In general, the average pore size of samples increases with increase in gravel content. When the gravel content is less than 50%, there is an approximately linear relationship between average pore size and gravel content of gravel soil. When the gravel content exceeds 50%, the average pore size of the samples increases significantly; especially the average pore size of samples with 80% gravel content is about 2.3–4.4 times that of samples with 20% gravel content.

As shown in Figure 12, during the loading process, when the gravel content is less than 60%, the average pore size of the gravel soils shows a V-shaped trend as the axial strain increases. The average pore size of samples with gravel content less than 40% decreases by 21.5–26.7% at the turning points, while the average pore size of samples with gravel content more than 40% decreases by 8–14% at the turning points. When the gravel content is more than 60%, the average pore size of gravel soils increases by 10–32.5% during the whole loading process.

Discussion

The variations of pore properties of gravel soils under different confining pressures and using the loading process are obtained by the above-mentioned numerical simulation. The reasons for the variations of pore properties are discussed below.

(1) As the amount of gravel increases, the porosity of the samples decreases first and then increases, while the average pore size always increases. Figure 13 shows the internal structure of samples with low content, medium and high gravel content. There are more fine particles in samples with low gravel content. Therefore, the average pore size between the particles is small. In samples with medium gravel content, with increase in particle radius, the size of pores between the particles also increases. However, these pores are filled by finer particles of gravel soils, and the porosity is reduced due to a more compact sample. The samples with high gravel content mainly consist of large-sized particles; the average size of pores between particles is large because of the lack of adequate fine particles to fill these pores.

(2) With the increase in confining pressure, the pores in the gravel soils are compressed. There is a decrease in both pore size and porosity. However, compressibility between the gravel particles is much smaller than that between the soil particles. Therefore, the decrease in porosity and average pore size in samples with higher gravel content is small. When the

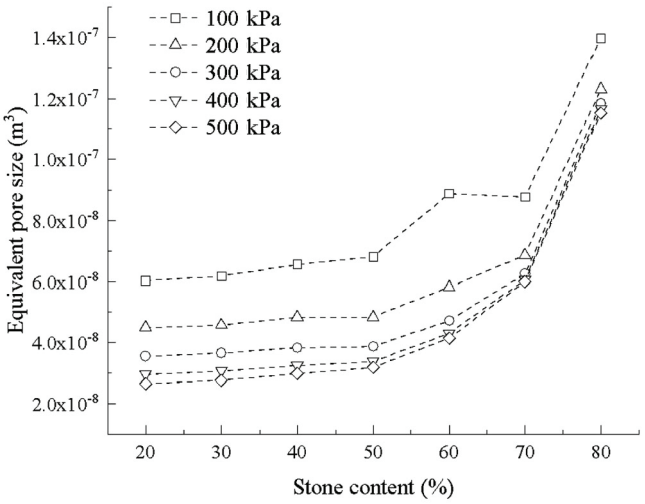

Figure 11. Relationship between equivalent pore size and gravel content.

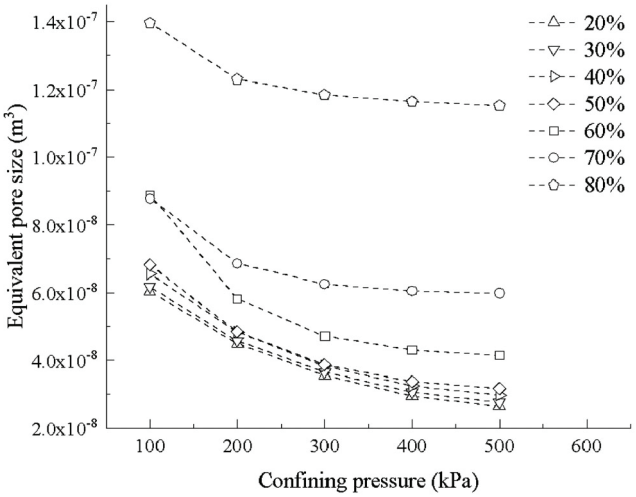

Figure 10. Relationship between equivalent pore size and confining pressure.

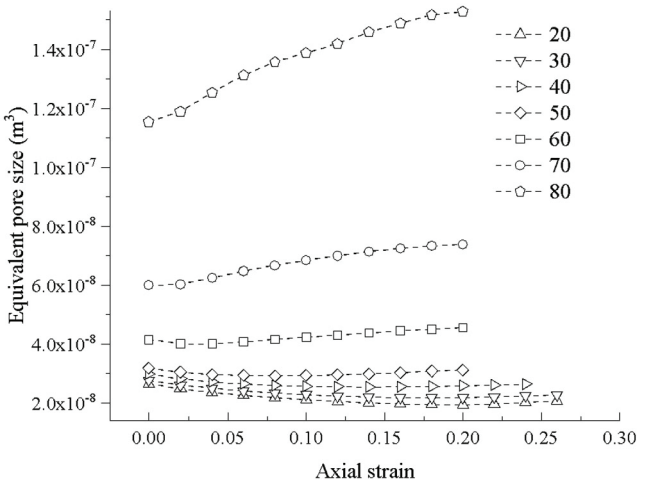

Figure 12. Relationship between equivalent pore size and axial strain.

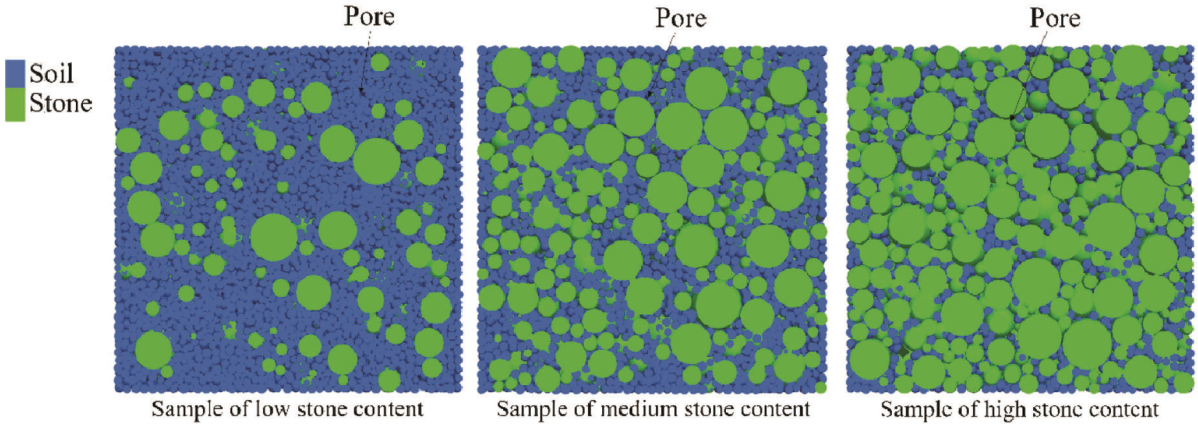

Figure 13. The internal structure of samples with different stone contents.

gravel content is less than 50%, the gravel particles in the samples are surrounded by soil particles and cannot make contact with each other. The pores between soil particles and gravel particles are compressed during the loading process. Therefore, the variations of pore properties of these samples are similar.

(3) During the loading process, the original structure of samples with high gravel content is destroyed, and dislocations of the gravel particles lead to increase in the gaps between particles. The average pore size and porosity of the samples increase accordingly. In samples with medium and low gravel content, the soil particles can be further compressed; the average pore size and porosity decrease before these samples are yielded. When the original structure of the soils and gravels is destroyed, the gap between these particles increases and there is an increase in porosity and average pore size as well.

Conclusion

The variations of the pore properties in gravel soil under triaxial compression have been studied. The following conclusions can be drawn by a numerical simulation of samples with seven different gravel contents.

(1) The gravel content has a major influence on the pore properties of gravel soil. The porosity of gravel soils shows a V-shaped trend with the gravel content, but the average pore size of samples increases with increase in gravel content. The samples of medium gravel content are most easily compacted.

(2) During the loading process, both porosity and average pore size of samples decrease first and then increase with increase in axial strain. The gravel soil samples have minimum porosity in the yield stage, which is an inherent property of the gravel soil.

1. Zhu, J.-G., Guo, W.-L., Wen, Y.-F., Yin, J.-H. and Zhou, C., New gradation equation and applicability for particle-size distributions of various soils. *Int. J. Geomech.*, 2018, **18**(2), 1–8.
2. Yu, J., Wang, R., Zhang, J., Yan, L., Meng, Q., Zhang, C. and Li, X., Deformational characteristics of Donglinxin slope induced by reservoir fluctuation and rainfall. *Curr. Sci.*, 2017, **113**(6), 1159–1166.
3. Conte, E., Donato, A. and Troncone, A., A simplified method for predicting rainfall-induced mobility of active landslides. *Landslides*, 2017, **14**(1), 35–45.
4. Liu, Y. and Jeng, D.-S., Pore structure of grain-size fractal granular material. *Materials*, 2019, **12**(13), 2053.
5. Chapuis, R. P. and Aubertin, M., On the use of the Kozeny Carman equation to predict the hydraulic conductivity of soils. *Can. Geotech. J.*, 2003, **40**(3), 616–628.
6. Jia, C., Yu, J., Zuo, J. and Eti-Inyenetrenchard, I., The creep behavior and permeability evolution of breccia lava in triaxial creep tests. *Géotech. Lett.*, 2019, **9**(1), 1–12.
7. Li, C., Yang, Y. T. and Hong, Z., Numerical study of soil–rock mixture: generation of random aggregate structure. *Sci. China Technol. Sci.*, 2018, **61**(3), 359–369.
8. Lopez, R. D. F., Silfwerbrand, J., Jelagin, D. and Birgisson, B., Force transmission and soil fabric of binary granular mixtures. *Géotechnique*, 2016, **66**(7), 1–6.
9. Jin, L., Zeng, Y. W. and Zhang, S., Large scale triaxial tests on effects of rock block proportion and shape on mechanical properties of cemented soil-rock mixture. *Rock Soil Mech.*, 2017, **38**(1), 141–149.
10. Wen-Jie, X., Qiang, X. and Rui-Lin, H., Study on the shear strength of soil–rock mixture by large scale direct shear test. *Int. J. Rock Mech. Min. Sci.*, 2011, **48**(8), 1235–1247.
11. Wen-Jie, X. U., Rui-Lin, H. U. and Wang, Y. P., PFC2D model for mesostructure of inhomogeneous geomaterial based on digital image processing. *J. China Coal Soc.*, 2007, **32**(4), 358–362.
12. Qiang, Z., Xu, W. Y., Liu, Q. Y. and Meng, Q. X., A novel non-overlapping approach to accurately represent 2D arbitrary particles for DEM modelling. *J. Central South Univ.*, 2017, **24**(1), 190–202.
13. Ferellec, J. and McDowell, G., Modelling realistic shape and particle inertia in DEM. *Géotechnique*, 2010, **60**(3), 227–232.
14. Yang, J., Sun, H., Xing, M., Wang, X. and Zheng, J., Numerical analysis of the failure process of soil–rock mixtures through computed tomography and PFC3D models. *Int. J. Coal Sci. Technol.*, 2018, **5**(2), 1–16.
15. Shi, C., Yang, W., Yang, J. and Chen, X., Calibration of micro-scaled mechanical parameters of granite based on a bonded-particle

model with 2D particle flow code. *Granular Matter*, 2019, **21**(2), 38.
16. Roozbahani, M. M., Borela, R. and Frost, J. D., Pore size distribution in granular material microstructure. *Materials*, 2017, **10**(11), 1237.
17. Russell, A., How water retention in fractal soils depends on particle and pore sizes, shapes, volumes and surface areas. *Géotechnique*, 2014, **64**(5), 379–390.
18. Cousins, T. A., Ghanbarian, B. and Daigle, H., Three-dimensional lattice Boltzmann simulations of single-phase permeability in random fractal porous media with rough pore–solid interface. *Trans. Porous Media*, 2018, **122**(3), 527–546.
19. Chen, X. *et al.*, A new model of pore structure typing based on fractal geometry. *Mar. Pet. Geol.*, 2018, **98**, 291–305.
20. Roozbahani, M. M., Graham-Brady, L. and Frost, J. D., Mechanical trapping of fine particles in a medium of mono-sized randomly packed spheres. *Int. J. Num. Anal. Methods Geomech.*, 2014, **38**(17), 1776–1791.
21. Al-Raoush, R., Thompson, K. and Willson, C. S., Comparison of network generation techniques for unconsolidated porous media. *Soil Sci. Soc. Am. J.*, 2003, **67**(6), 1687–1700.
22. Rabbani, A., Ayatollahi, S., Kharrat, R. and Dashti, N., Estimation of 3-D pore network coordination number of rocks from watershed segmentation of a single 2-D image. *Adv. Water Resour.*, 2016, **94**, 264–277.
23. Medley, E., The engineering characterization of melanges and similar block-in-matrix rocks (bimrocks). Thesis, University of California, Berkeley, USA, 1994.
24. Nishiyama, N. and Yokoyama, T., Permeability of porous media: role of the critical pore size. *J. Geophys. Res.: Solid Earth*, 2017, **122**(9), 6955–6971.

ACKNOWLEDGEMENT. This work is financially supported by the National Key Research and Development Programme of China (grant no. 2017YFC1501100), National Natural Science Foundation of China (52008403) and the Jiangsu Natural Science Foundation of Youth, China (BK20180954).

Received 24 April 2020; revised accepted 29 July 2021

doi: 10.18520/cs/v121/i6/801-809